

ANL/ES/CP-97068

**INVESTIGATION OF PARTICLE/GAS FLOW  
CHARACTERISTICS IN PIPELINES\***

B. Golchert, S. L. Chang, and M. Petrick

Energy Systems Division  
Argonne National Laboratory  
Argonne, IL 60439

RECEIVED  
SEP 28 1999  
OSTI

June 1999

The submitted manuscript has been authored by a contractor of the U. S. Government under contract No. W-31-109-ENG-38. Accordingly, the U. S. Government retains a nonexclusive, royalty-free license to publish or reproduce the published form of this contribution, or allow others to do so, for U. S. Government purposes.

Submitted for publication in the  
1999 AIChE Symposium Series for Fluidization and Fluid Particle Systems, a paper selected from the  
"Advanced Technologies for Fluid-Particle Systems, Symposium B," and presented at the  
1998 AIChE Annual Meeting, Topical Conference on Advanced Technologies for Particle Processing  
Nov. 15-20, 1998, Miami, FL

---

\*Work supported by the U.S. Steel Corporation.

## **DISCLAIMER**

**This report was prepared as an account of work sponsored by an agency of the United States Government. Neither the United States Government nor any agency thereof, nor any of their employees, make any warranty, express or implied, or assumes any legal liability or responsibility for the accuracy, completeness, or usefulness of any information, apparatus, product, or process disclosed, or represents that its use would not infringe privately owned rights. Reference herein to any specific commercial product, process, or service by trade name, trademark, manufacturer, or otherwise does not necessarily constitute or imply its endorsement, recommendation, or favoring by the United States Government or any agency thereof. The views and opinions of authors expressed herein do not necessarily state or reflect those of the United States Government or any agency thereof.**

## **DISCLAIMER**

**Portions of this document may be illegible in electronic image products. Images are produced from the best available original document.**

# INVESTIGATION OF PARTICLE/GAS FLOW CHARACTERISTICS IN PIPELINES

B. Golchert, S. L. Chang, and M. Petrick, Energy Systems Division  
Argonne National Laboratory, Argonne, IL 60439

## INTRODUCTION

Gas-solid flows occur frequently in many industrial processes and systems, such as in pulverized coal transport pipelines and portions of fluid catalytic cracking (FCC) risers. Many of these systems have been modeled and optimized over the years by "engineering know-how," which has been derived from the operating experience with the unit. However, it is being recognized that a more detailed, analytic tool is necessary to improve the efficiency of these systems due to heightened industrial competitiveness. In addition to this competition, increasingly stringent environmental regulations force the industry to improve their systems to comply with these regulations.

In part, these two conditions explain the recent interest in computational fluid dynamics (CFD) applied to industrial systems. A successfully validated CFD simulation can provide detailed information on an industrial flow system based on a limited amount of experimental data. Once a CFD code has been properly validated, it may then be used to suggest optimal operating conditions. Given the wide range of information provided by a CFD code, the term "optimal" may refer to optimal material output, optimal energy efficiency, minimal (optimal) pollutant emission, or optimal lowest operating cost, for example. This versatility has been recently recognized by a number of industries (for example, refinery, chemical, aluminum, and glass), all of which have identified CFD as a critical field for advancement of their technology.

The ultimate goal of applying CFD to the modeling of an industrial system is to produce meaningful data that may be used by the company to improve plant performance. The amount of useable data partially depends on how the system is numerically modeled. Any physical system may be modeled by a Eulerian or Lagrangian approach (or a mixture of the two for multi-phase systems). Most of the recent work in modeling gas-solid flows is based on a Lagrangian model for the solid phase [Dasgupta, S. et. al., 1997], [Hrenya, C.M., and J.L. Sinclair, 1997], [Lun, C.K.K, and H.S. Liu, 1997], [Shirokar, J.S. et. al., 1996], [Tashiro, H., and Y. Tomita, 1991]. While this approach models the physics of the system on a microscopic level very well, it is often difficult to extract engineering system information from a Lagrangian formulation. This thought has been re-confirmed in a recent paper: "...the particle paths which result from a Lagrangian description often do not contain enough information for engineers" [Tu, J.Y., et. al. 1998]. Therefore, a Eulerian approach was used in this code to model all phases of the system. After validation of the code, it was seen that the Eulerian approach provided information needed to improve a coal transfer system.

## NUMERICAL APPROACH

Over the years, the ICRKFLO code was developed at Argonne National Laboratory (ANL) by expanding and enhancing an existing multi-phase reacting flow computer code. The computer code was originally a general CFD code numerically solving conservation equations of mass, momentum, and energy for multi-phase flows on a staggered grid. Recently, for simulating an FCC riser flow, new features were added to the code, which include a model for particle-solid interactions. This enhancement is directly applicable to the study of a pulverized coal transport pipeline system.

### Governing Equations

ICRFLO solves the conservation equations of general flow properties for three phases: gaseous species, liquid droplets, and solid particles. General conservation laws, expressed by elliptic-type partial differential equations, are used in conjunction with rate equations governing the mass, momentum, enthalpy, and species for a three-phase flow with gas species, liquid droplets, and solid particles. For this study, only the solid and gaseous phases are present in a two-dimensional flow. Governing equations include the equation of state and the continuity and the momentum equations. Two additional transport equations are needed for solving the turbulent diffusivity. For convenience in numerical formulation, the governing conservation/transport equations for the gas phase are put in a common form, Eq. (1):

$$\frac{\partial}{\partial x}(\theta \rho u \xi - \Gamma_{\xi} \frac{\partial \xi}{\partial x}) + \frac{\partial}{\partial y}(\theta \rho v \xi - \Gamma_{\xi} \frac{\partial \xi}{\partial y}) = S_{\xi} \quad (1)$$

in which  $\xi$  is a general gas flow property (scalar, velocity components, turbulent kinetic energy, and turbulent dissipation rate);  $x$  and  $y$  are spatial coordinates;  $\theta$  is the gas volume fraction;  $u$ ,  $v$  are velocity components;  $\Gamma$  is an effective diffusivity (calculated from both laminar and turbulent diffusivities); and  $S_{\xi}$  is the sum of source terms applicable to that equation.

The particle phase formulation is derived from a Eulerian approach. In this formulation, the state of the particle-phase flow is governed by the elliptic partial differential equations of fluid mechanics, including conservation of particle

number density, and momentum. Particles are generally divided into various groups according to their sizes. Similar to the gas phase formulation, the governing transport equations for the particle phase of the  $k^{\text{th}}$  size group is put in a common form, Eq. (2):

$$\frac{\partial}{\partial x}(n_k u_{c,k} \xi - \Gamma_\xi \frac{\partial n_k \xi}{\partial x}) + \frac{\partial}{\partial y}(n_k v_{c,k} \xi - \Gamma_\xi \frac{\partial n_k \xi}{\partial y}) = S_\xi \quad (2)$$

in which  $\xi$  is the general particle flow property (number density, x- and y-momentum);  $n_k$  is the particle number density of  $k^{\text{th}}$  size group;  $u_{c,k}$  and  $v_{c,k}$  are the particle velocity components of  $k^{\text{th}}$  size group in the x and y direction, respectively;  $\Gamma$  is the particle diffusivity resulting from interaction with turbulence in the gas phase; and  $S_\xi$  is the sum of source terms for each equation. The formulation of the computer code allows for a size spectrum of particles; however, in this study, only one size group of particles was used. The use of mono-sized particles was considered a reasonable first step in utilizing a two-phase flow model to analyze the system.

The momentum equations contain source terms for interphase and intraphase property exchange rates. The computation of these rates may, in some cases, be based on rather elaborate models, which resolve or avoid the numerical instabilities arising out of widely disparate time scales in the macro- and micro-physical scales. Several phenomenological models have been employed to numerically represent these important effects that drive the two-phase flow. The models involve particle-solid interactions, interfacial drag, and multiphase turbulence.

### Particle-Solid Interaction Model

In a dilute multiphase flow, the particles generally follow with the gas flow. In a dense multiphase flow, particle-particle and particle-wall interactions become significant and can cause a redistribution of the particles. Experimental data show a U-shaped particle number density distribution in a cross-section of those pipelines with upflow or downflow. The particle number density is an important phenomenon to model properly since it strongly influences the effectiveness of a unit, such as a FCC riser, where the particle number density influences reaction rate and heat transfer. Multiphase hydrodynamic CFD codes have difficulty describing such a U-shape distribution due to the lack of a proper model for particle-solid interactions. A new particle-solid interaction model has been developed. This model accounts for particle-particle and particle-wall collisions in regions of high particle volume fraction. Solid diffusivity and solid stress terms are added to the source terms of the momentum equations. The ICRKFLO code uses this new model in calculations that duplicate the observed U-shape distribution.

In a dense flow region, a moving particle tends to collide with neighboring particles, and the collisions cause the particles to diffuse across the flow stream. Since the particle diffusion process is similar to that of gas molecules, a solid diffusivity can be derived. Since particle collision frequency is proportional to local particle mass flux, the solid diffusivity can be derived as:

$$S_{sd,x} = \mu_{sd} \frac{\partial (nv_s)}{\partial x} \quad (3)$$

The term, Eq.(3), is added to the particle x-momentum equation to account for the diffusion due to particle-particle collisions. A similar term can be derived for the particle y-momentum equation.

Sometimes, particles are packed in locations where the particle velocity is low. When particles are packed, a particle exerts a force directly on the neighboring particles. A solid stress term is defined for this packed situation. The solid stress is assumed to be proportional to the local solid volume fraction, provided the solid fraction exceeds a preset packed value.

$$S_{sp,x} = \frac{\partial}{\partial x} [\kappa(\theta_s - \theta_{sp})] \quad \text{if } \theta_s > \theta_{sp} \quad (4)$$

This term, Eq.(4), can be added to the particle momentum equation, and it will only contribute when the particle volume fraction is greater than a pre-set maximum. But, this approach can easily cause numerical divergence because a small change in the calculated solid volume fraction results in a huge change in the solid stress. A better approach, which is used here, is to accumulate local solid stress and calculate solid volume fraction from the solid stress.

### Interfacial Drag Model

In a multiphase flow, particles are driven by the gas flow through the drag force. The drag force is caused by the velocity difference between the gas and solid phases ( $u_s$ , called slip velocity). Empirical drag equations have been commonly used. For a single particle in the gas flow, the drag force of gas exerted on the particle is expressed as a function of the slip velocity kinetic energy, the particle's cross-sectional area, and an empirical drag coefficient. The particle drag force is in the same direction as the slip velocity. The direction of the drag force depends on the sign of the slip velocity. The drag coefficient,  $C_d$ , is generally represented by the Reynolds number  $Re_s$ .

$$C_d = \frac{24 (1 + 0.15 \text{Re}_s^{0.687})}{\text{Re}_s} \quad \text{and} \quad \text{Re}_s = \frac{2\rho |u_g| r}{\mu} \quad (5)$$

Not including the collisions between particles, the drag force of the gas on a collection of particles can be obtained by summing up the drag force on the individual particles. Integrating over particle size space for a particle size group, the drag force exerted by the gas on the particles of the  $i^{\text{th}}$  size lump is shown in Eq. (6). This drag force is the source term  $S_{u,i}$  of the particle x-momentum equation.

$$S_{u,i} = C_{d,i} \rho |u_{g,i}| u_{g,i} \frac{\pi r_i^2}{2} n_i \quad (6)$$

The interfacial drag forces of the particles and the gas are conserved if the friction dissipation on the particle surface is negligible. The drag force on the gas should be balanced by the drag force on the particles. Therefore, the drag force on the gas can be obtained by summing the particle drag terms over all particle size groups, and it becomes a source term for the gas momentum equation. In a similar way, source terms of the y-direction drag force can be derived for the particle and gas momentum equations.

### Multiphase Turbulence Model

A multiphase k- $\epsilon$  model [Zhou and Chiu, 1983] is used in this study. The k- $\epsilon$  model was modified for multiphase flows to account for the turbulent dispersion of particles. The multiphase turbulent transport equations are derived from the single-phase turbulence transport equations by adding a void fraction to the density terms and sink terms in the equations. A sink term is added to the k-equation to account for the loss rate of turbulent kinetic energy in the gas phase as this energy is transferred to particles in the turbulent dispersion process. The loss of the turbulent kinetic energy depends on the particle size. If the particle size is in the sub-micrometer range, the particles can dissipate the turbulence kinetic energy as effectively as the gas, and the loss rate is set to the gas phase kinetic energy convective rate. If the particle size is larger than 100  $\mu\text{m}$ , the loss of turbulent kinetic energy becomes negligible. Particle diffusivity also depends on the particle size. For particles larger than 100  $\mu\text{m}$ , turbulent fluctuations (eddies) have little effect on them and their momentum is only affected by drag computed from the mean gas flow. If the particle size is in a sub-micrometer range, the particles move along with gas flow and have a similar turbulent diffusion effect as the gas phase.

### APPLICATIONS TO A PULVERIZED COAL TRANSFER PIPELINE

This section of the paper presents results from the application of ICRKFLO to a pulverized coal transfer pipeline. These results will give a strong indication of the utility of this code for analyzing and improving two-phase flow systems. The coal transport system between storage bins and a blast furnace consists of a series of long pipes of various lengths, orientation, and flow characteristics. Figure 1 depicts the computational configuration used to model the transfer pipeline. The coal storage bin is located at point A and the blast furnace is located at point H. The points A through H are used to define individual segments of the system.

A majority of the length of this system consists of horizontal flow. It is expected that in these regions there will be some settling of the coal particles (due to gravity), thus creating a stratified flow with coal particles on the bottom and carrier gas on the top. In addition to this settling on the horizontal sections, coal pileup is expected to occur in the elbows where the pileup is caused by the slow response of the particles to the change of flow direction.

It is this change in flow direction in the elbows that creates additional numerical complications when modeling this pipeline. Some of the particles flowing into the elbow will impact upon the curved wall and may adhere or stay near the wall. When a large number of particles begin to reside in the same location, this effect is referred to as pileup. As particles begin to pile up, their presence begins to restrict the effective flow area in the pipe, thus leading to higher velocities and larger pressure drops. The flow patterns inside the elbow will be different depending upon the inlet and outlet piping orientation (horizontal/vertical inlets and outlets).

Once the particles have settled near the wall, they do not numerically "stick" to the wall. Rather, they will stay near the wall until a strong enough force is present to pull them away from the wall. The only forces acting in this system are the force of gravity and the drag force exerted by the moving gas. As was mentioned earlier, the drag force is proportional to the velocity of the gas. Thus, if the gas velocity is low (as it is near the walls of the pipe), the drag force is low. This implies that there is only a weak force trying to pull the particles back into the center regions of the pipe. In reality, this is a transient problem, but because pileup is a rather slow process (on the order of weeks or months for an industrial system), the problem may be treated as steady state.

The flow through these elbows was modeled by ICRKFLO as part of the sectional modeling approach [Chang et al., 1996]. Several different inlet conditions to the elbows were examined, and the results generated reflect the flow patterns found in industry. The first elbow encountered in the flow system changes downflow into horizontal flow. The particle number density was not as stratified for this first elbow as it will be for later elbows. However, even for this first

elbow, Figure 2 indicates that there will be some particle pileup. Since the flow is not very stratified, the pileup is not as severe as that in other elbows. The gas flow field follows the curve of the elbow (results not pictured), while Figure 2 reveals that the particles tend to follow straight lines until they impact on the elbow walls.

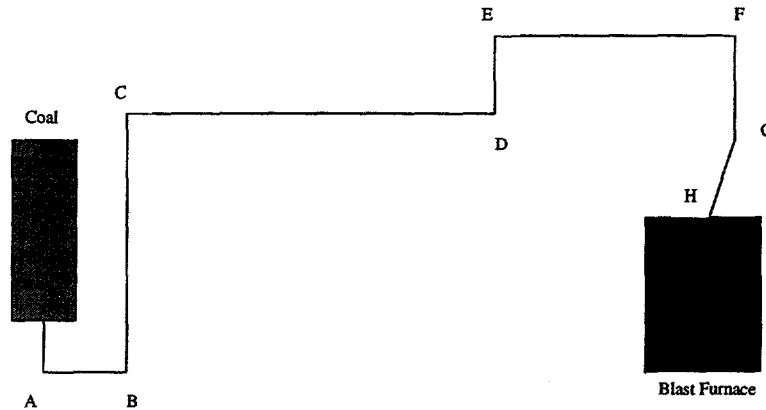


Figure 1: Configuration of a Sample Coal Transport Pipeline

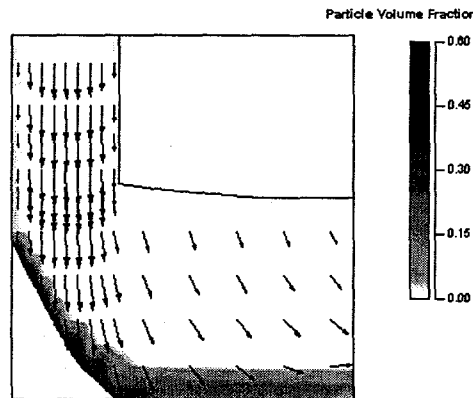


Figure 2: Elbow Turning Down Flow into Horizontal Flow (Particle Velocity Shown)

It is appropriate at this point to note that all of the calculations were done in steady state, even though the actual system is transient. Thus, all of the results from this work are brief “snapshots” of the system. The particle pileup in these figures represents an equilibrium condition. For a converged numerical result, every coal particle that enters the regions of high particle number density kicks out another coal particle back into the flow stream. The total number of particles packed in the system is therefore unchanging.

As was previously mentioned, a CFD code applied to an industrial system should give indications on how to improve the performance of the system. If a CFD code indicates where the particles would pile up in a coal transfer system, then the system designer would know the most likely locations where the pipeline would clog. Figure 3 is a plot of the particle volume fraction for the bottom side of the pipe and for the top side of the pipe. By bottom side, it is meant that radius of the pipe that is farthest “down” in the gravitational direction.

The peaks in Figure 3 represent those locations where the particle packing is high. The black line indicates the bottom surface, and it is on this surface that pileup is expected since gravity will cause the coal particles to settle on the lower surface. The first two peaks on the black line in Figure 3 represent the pileup at the elbow between segments AB and BC and at the elbow between segments BC and CD. Between these two peaks, the particle volume fraction on the bottom surface is larger than the particle volume fraction on the top surface. This indicates that the particles are settling. The section between the two black peaks is segment BC, a horizontal segment. In this region, the heavier coal particles will settle to the bottom surface because of the pull of gravity. This causes more coal particles to be near the bottom surface with more gas flow near the top surface.

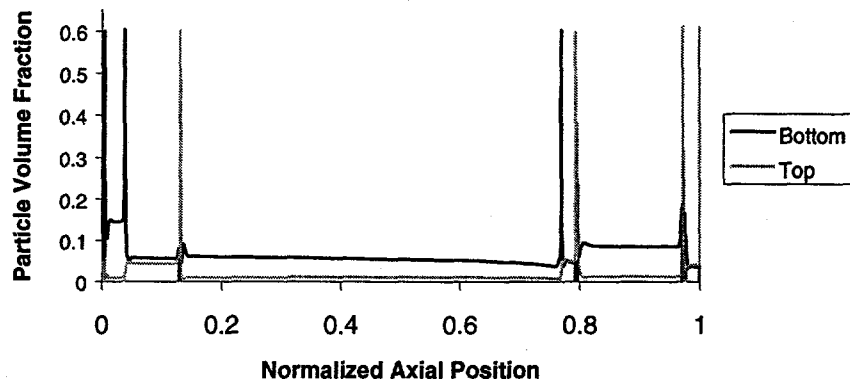


Figure 3: Particle Volume Fraction as a Function of Position along Coal Transport System

Between the second black peak and the first gray peak is segment CD (upflow). With upflow (and downflow), the particle number density distribution (particle volume fraction) is expected to be annular, with both walls of the annulus having approximately the same particle volume fraction. This is evidenced by the black and the gray lines between the two peaks being nearly equal. The bottom particle volume fraction (lower side of the pipe) is slightly higher than the top particle volume fraction due to the increased particle volume fraction on the bottom surface at the entrance to segment CD. The third peak is gray because the coal particles in upflow impinge upon the top wall of the pipe and begin to pile up.

Thus, all of the peaks in Figure 3 may be explained as either particle pileup in an elbow (a black peak) or particle impingement causing pileup (a gray peak). The particle pileup in the elbows represent a serious concern since there is no force present to remove this pileup. The pileup caused by impingement is continually being pulled down by gravity, but the particles are constantly being forced back into the elbow by the impingement of the main flow of particles.

Of all the locations of particle packing, the most serious location is the elbow between segments DE and EF. This elbow occurs at the end of an extremely long horizontal segment. In this segment, the coal particles will settle to the bottom radius of the pipe, and the gas will flow along the top radius of the pipe. This stratification before the elbow will slow down the coal particles. When these slower particles hit the elbow, there is much less force (pressure) present to lift them out of the elbow. Along section DE, more than fifty percent of the total system pressure drop is lost. In addition, segment EF is upflow so the particles must move against the force of gravity. This combination of stratified flow, loss of system pressure, and upflow creates a situation that is difficult to model numerically.

To test the validity of the model, ICRKFLO was set and run for a set of industrial conditions provided by US Steel. The calculated pressure drops were compared with the experimental pressure drop measurements, as can be seen in Figure 4. The agreement between the calculations and the measurements is very good.

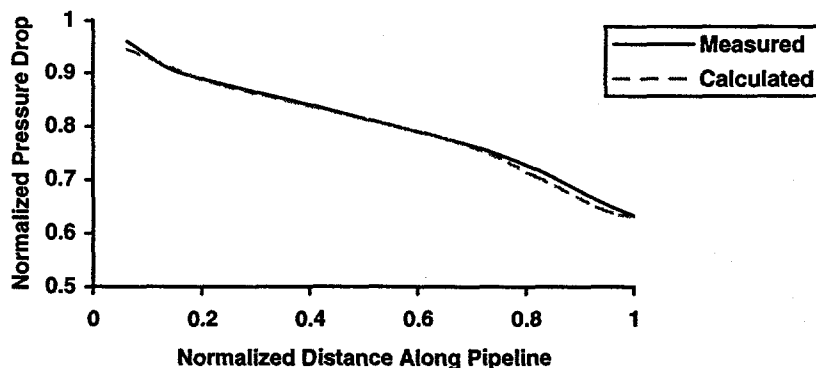


Figure 4: Measured and Calculated Pressure Drop along Pipeline

By using the validated code, a parametric study was performed to determine the effects of operating parameters on the system's performance. The two main parameters that were examined were the coal mass flow rate and the average size of the coal particles. The code shows that with increased particle mass flow rate, the pressure drop for each segment increases. The increased flow rate also increases the pileup in the elbows. Also, the particle volume fraction was found to be affected by the size of the particle. The larger particles tend to pack more readily than the smaller particles, and this phenomenon is also reflected in the computations.

## CONCLUSIONS

Improved models have been incorporated into ICRKFLO to better model gas-solid flows. These Eulerian models have been applied to industrial pipeline systems. ICRKFLO correctly reproduces the annual flow expected in upflow and downflow conditions, while the code also properly models the particle settling in horizontal flow. Increased particle mass flow rate and increased average particle size will increase the likelihood of particle pileup. Finally, comparison between ICRKFLO calculations and system pressure measurements show an exceptionally good agreement. The results clearly indicate that ICRKFLO is quite capable of modeling these dense two-phase flow systems. Once validated against industrial measurements, the code may then be used as a tool to improve the performance of the gas-solid system.

## ACKNOWLEDGMENTS

The authors would like to thank the U.S. Steel Corporation for its support of this work. The authors would also like to gratefully acknowledge the assistance of Professor Chenn Zhou (Purdue Univ.-Calumet) and Dr. Steven Lottes (ANL).

## REFERENCES

Chang, S.L., C.Q. Zhou, S.A. Lottes, J. X. Bouillard, and M. Petrick, "A Sectional Coupling Approach for the Simulation of Multi-Phase Reacting Flow in a Bent Reactor," *HTD-Vol. 335, Proc. of the ASME Heat Transfer Division* 4:361-373, International Mechanical Engineering Congress and Exposition, Atlanta, GA (November 17-22, 1996).

Dasgupta, S., R. Jackson, and S. Sundaresan, "Developing Flow of Gas-Particle Mixtures in Vertical Ducts," *Ind. Eng. Chem. Res.*, 36:3375-3390 (1997).

Hrenya, C.M., and J.L. Sinclair, "Effects of Particle-Phase Turbulence in Gas-Solid Flows," *AICHE Journal*, Vol. 43, No. 4, April (1997).

Lun, C.K.K., and H.S. Liu, "Numerical Simulation of Dilute Turbulent Gas-Solid Flows in Horizontal Channels," *Int. Journal of Multiphase Flow*, 23(3):575-605 (1997).

Shirokar, J.S., C.F.M. Coimbra, and M.Q. McQuay, "Fundamental Aspects of Modeling Turbulent Particle Dispersion in Dilute Flows," *Prog. Energy Combustion Sci.*, 22:363-399 (1996).

Tashiro, H., and Y. Tomita, "A Numerical Simulation for Gas-Solid Two-Phase Flow (Influence of the Collision between Particles on the Vertical Upward Flow)," *JSME International Journal, Series II*, 34(2):129-133 (1991).

Tu, J.Y., C.A.J. Fletcher, Y.S. Morsi, W. Yang, and M. Behnia, "Numerical and Experimental Studies of Turbulent Particle-laden Gas Flow in an In-line Tube Bank," *Chemical Engineering Science*, 53(2):225-238 (1998).

Zhou, X.Q., and H.H. Chiu, "Spray Group Combustion Processes in Air Breathing Propulsion Combustors," *AIAA/SAE/ASME 19<sup>th</sup> Joint Propulsion Conference*, Washington, AIAA-83-1323 (1983).